Histol Histopathol (2024) 39: 715-727

Histology and Histopathology
From Cell Biology to Tissue Engineering

ORIGINAL ARTICLE Open Access

Differential expression of WNT5A long and short isoforms in non-muscle-invasive bladder urothelial carcinoma

Amy M. Strope[1], Cody Phillips[1], Sabin Khadgi[1], Scott A. Jenkinson[2], Karen T. Coschigano[1]* and Ramiro Malgor[1]*

[1]Department of Biomedical Sciences, Heritage College of Osteopathic Medicine, Ohio University and [2]OhioHealth O'Bleness Laboratory Services, O'Bleness Hospital, Athens, Ohio, USA

*These authors are joint senior authors

Summary. Wnt ligands belong to a family of secreted glycoproteins in which binding to a range of receptors/co-receptors activates several intracellular pathways. WNT5A, a member of the Wnt family, is classified as a non-canonical Wnt whose activation triggers planar cell polarity (PCP) and Ca^{+2} downstream pathways. Aberrant expression of WNT5A has been shown to play both protective and harmful roles in an array of conditions, such as inflammatory disease and cancer.

In the present study, using histological, immuno-histochemical, and molecular methods, we investigated the expression of two isoforms of WNT5A, WNT5A-Short (WNT5A-S) and WNT5A-Long (WNT5A-L) in bladder urothelial carcinoma (UC). Three UC cell lines (RT4, J82, and T24), as well as a normal urothelial cell line, and formalin-fixed, paraffin-embedded (FFPE) transurethral resection (TUR) tissue samples from 17 patients diagnosed with UC were included in the study. WNT5A-L was the predominantly expressed isoform in urothelial cells, although WNT5A-S was also detectable. Further, although no statistically significant difference was found between the percentage of WNT5A-S transcripts in low-grade *versus* high-grade tumors, we did find a difference between the percentage of WNT5A-S transcripts found in non-invasion *versus* invasion of the lamina propria, subgroups of non-muscle-invasive tumors.

In conclusion, both WNT5A-S and WNT5A-L isoforms are expressed in UC, and the percentage of their expression levels suggests that a higher proportion of WNT5A-S transcription may be associated with lamina propria invasion, a process preceding muscle invasion.

Corresponding Author: Ramiro Malgor, MD, Department of Biomedical Sciences, 220b Academic and Research Center, Ohio University, Athens, OH 45701, USA. e-mail: malgor@ohio.edu

www.hh.um.es. DOI: 10.14670/HH-18-723

Key words: Biomarker, Bladder urothelial carcinoma, WNT5A, WNT5A isoforms, Wnt signaling

Introduction

Wnt ligands belong to a large family of secreted glycoproteins that bind to a broad spectrum of receptors/co-receptors and turn on a variety of intracellular pathways. Wnt signaling activation is dependent on the receptor context expressed by the target cells and works in an autocrine or paracrine manner (Mikels and Nusse, 2006b; Hausmann et al., 2007). A broad range of receptors and co-receptors, including Frizzled (FZD) family receptors, low-density lipoprotein receptor-related protein (LRP), the receptor tyrosine kinase-like orphan receptor family (ROR 1 /2), and the related receptor tyrosine kinase (RYK), can bind Wnt ligands (Gordon and Nusse, 2006). Wnt pathways are complex, traditionally divided into canonical or β-catenin-dependent, which are better studied and known, and non-canonical or β-catenin-independent, which are still poorly understood. Wnt pathways are evolutionarily conserved, playing critical roles in embryonic development and tissue homeostasis by regulating various cell functions, such as differentiation, proliferation, migration, polarity, and apoptosis (Mikels and Nusse, 2006b). Interestingly, altered expression of Wnt proteins and activation of Wnt pathways have been reported in several pathological processes (Pukrop et al., 2006; Geng et al., 2012; Bo et al., 2013; Ackers et al., 2020), This peculiarity has made Wnt signaling an interesting and challenging topic to study as a potential diagnostic or therapeutic target (Barker and Clevers 2006; Le et al., 2015; Ng et al., 2019).

WNT5A is a member of the Wnt family, classified as a non-canonical Wnt, whose activation results in activation of planar cell polarity (PCP) and Ca^{+2}

downstream pathways (Mikels and Nusse, 2006a). However, it has also been shown that WNT5A activates a canonical signaling pathway (Mikels and Nusse, 2006a). Aberrant expression of WNT5A has been shown to play both protective and harmful roles in an array of conditions, including inflammatory conditions and various cancers (Blumenthal et al., 2006; Bhatt and Malgor 2014; Kumawat and Gosens 2016; Chen et al., 2021). In cancer specifically, WNT5A has been shown to exhibit either tumor suppressor or tumor promoter effects, depending on the type of cancer (McDonald and Silver 2009; Azbazdar et al., 2021). The role of WNT5A in different steps during tumorigenesis and metastasis has been reported, and several reviews have been published on this subject (Asem et al., 2016; Kumawat and Gosens, 2016).

Bladder cancer ranks 12th among all types of cancer when both sexes are considered; however, it is the fourth most common cancer in men, accounting worldwide for 573,278 new cases and 212,536 deaths in 2020 (Sung et al., 2021). In the U.S., 82,290 new cases were estimated for 2023, 62,420 cases for males and 19,870 for females, with 16,710 estimated deaths for the same year (Siegel et al., 2023). Urothelial carcinoma (UC), which constitutes more than 90-95% of all primary bladder cancers, is clinically divided for therapeutic and prognosis purposes into three disease states: non-muscle-invasive, muscle-invasive, and metastatic (Miyazaki and Nishiyama, 2017). Currently, UC diagnosis is based on cystoscopic examination of the bladder and histological evaluation of resected tissue, with histologic grading and depth of tumor invasion being the most important prognostic factors (Powles et al., 2022). Using the WHO 2016 histologic classification system, the non-muscle-invasive UC category is comprised of two stages, pTa or non-invasive tumors and pT1 or lamina propria-invasive tumors. The muscle-invasive category includes pT2 or muscularis propria-invasive and higher tumor stages (pT3, pT4) (Humphrey et al., 2016; Magers et al., 2019). The initial diagnosis in 75% of UC cases presents as low histological grade and stage, i.e., non-invasive pTa or pT1 stage, which in 50-70% of cases recurs after the first transurethral resection of the urinary bladder tumor (TURBT) but rarely progresses to invasion. The first diagnosis of the other 25% of cases is split roughly evenly between those presenting with muscle-invasive pT2 stage or higher and those presenting with metastases, both of which require more drastic treatments (Powles et al., 2022; Hasan et al., 2023; Santini et al., 2023). The diagnosis of UC, and hence its prognostic outcome and treatment, is a challenge due to its wide spectrum of histological variants. Although there have been numerous studies investigating the use of biomarkers for the identification of different histological variants and categories of UC, there is not yet consensus on their clinical application, with histopathological examination remaining the gold standard technique (Powles et al., 2022).

Involvement of canonical WNT, or the β-catenin-dependent pathway, in UC has been reported (Urakami et al., 2006; Costa et al., 2010; Garg and Maurya, 2019) but few studies have been published about the role of the non-canonical/β-catenin-independent WNT pathway. In this context, we previously reported a positive correlation between WNT5A protein and RNA expression and histological tumor grade in human UC tissue samples and showed that WNT5A increased cell migration in UC cell lines (Malgor et al., 2013; Saling et al., 2017). Additionally, Cao et al. (2018) reported that knockdown of Wnt5a expression reversed resistance to gemcitabine, a nucleoside analog used to treat muscle-invasive or metastatic bladder cancer (Cao et al., 2018). Thus, Wnt5a appears to play a tumor-promoting role in UC.

The novel discovery of two isoforms of WNT5A opened doors to speculation about the possible involvement of these two isoforms in the contradictory and opposing roles of WNT5A in different cell types and different types of cancers. The two WNT5A isoforms, named WNT5A-L (Long or A) and WNT5A-S (Short or B), are produced by alternative splicing of two different first exons, which is regulated by two independent promoters (Katoh and Katoh, 2009; Katula et al., 2012). The only structural difference between the encoded proteins is that WNT5A-S is truncated at the amino-terminal end, rendering it shorter than WNT5A-L, with 319 amino acids *versus* 337 amino acids, respectively (Bauer et al., 2013). The expression of isoform transcripts relative to each other differs by cell type (Bauer et al., 2013; Vaidya et al., 2016). Finally, several studies have shown that the isoforms have different roles, also depending on cell type (Bauer et al., 2013; Huang et al., 2017; Bhandari et al., 2021).

The current study aimed to quantify the RNA expression of the WNT5A-S and WNT5A-L isoforms in UC and normal bladder cell lines as well as in human UC tumor samples obtained by transurethral resection (TUR). We hypothesized that differential expression of the isoforms would correlate with specific histopathological features of the UC. In this manner, new diagnostic or therapeutic targets might be identified for UC.

Materials and methods

Cell line analysis

All *in vitro* studies were performed using three human neoplastic UC cell lines: T24 (HTB-4™), J82 (HTB-1™), and RT4 (HTB-2™) from the American Type Culture Collection (ATCC, Manassas, VA). These three cell lines were chosen because, although they are all adherent epithelial cells from the urinary bladder, RT4 was isolated from a transitional cell papilloma (benign lesion), while T24 and J82 were derived from high-grade UC. Interestingly, according to our previous report, cell lines T24 and J82 have different WNT5A expression levels (Saling et al., 2017). We also included

normal human bladder epithelial cells (NUC), from Lifeline Cell Technology #FC-0040 (Frederick, MD), as a control in the study. All cells were grown in the lab according to the manufacturer's instructions.

Total RNA for each cell line was isolated using TRIzol Reagent (Invitrogen, Carlsbad, CA) from separate cultures grown to 80% confluence in six-well plates. After the use of a Clean and Concentrate-5 Kit with DNase treatment (Zymo Research, Irvine, CA), RNA was quantified using a NanoDrop 2000 Spectrophotometer (Thermo Scientific, Waltham, MA).

Up to 1000 ng of RNA was reverse transcribed and amplified in either 44 µL or 15 µL reactions performed in duplicate using gene-specific probe degradation assays with specially designed primers and probes for each isoform (Table 1) (Integrated DNA Technologies, Inc., Coralville, IA), QIAcuity One-Step Viral RT-PCR kit, QIAcuity 24-well 26k or 96-well 8k Nanoplates, and a program of 50°C for 30 min, 95°C for 2 min and 40 cycles of 95°C for 5 sec, 55°C for 1 min in a QIAcuity One 5plex digital PCR system (QIAGEN, Germantown, MD). Results are presented as the mean of five separate cultures per cell line, normalized against the amount of total RNA added to each reaction.

Tissue sample selection

Archived formalin-fixed, paraffin-embedded (FFPE) TUR tissue samples from 17 patients diagnosed with UC (n=11 high grade and n=6 low grade) were obtained from the archives of the Pathology lab, O'Bleness Hospital OhioHealth (Athens, OH). All tissue samples were submitted for diagnostic purposes and the study was conducted according to ethical principles approved by Ohio University IRB protocol #07E112. All histological diagnoses were reviewed before inclusion in the study and tumors were staged using WHO/ISUP consensus criteria (Humphrey et al., 2016). The pathology reports are summarized in Table 2. For the study, consecutive sections were prepared for the assays. In brief, FFPE samples were cut into 4-µm-thick sections for Hematoxylin and Eosin (HE) staining, immunohistochemistry (IHC), and *in situ* hybridization (ISH); another 10-µm-thick section was cut for laser microdissection (LMD). HE staining was performed using a standard automated protocol at the Ohio University histology core facility.

Immunohistochemistry (IHC)

IHC for total/pan WNT5A was performed using mouse IgG1 monoclonal anti-human WNT5A clone 3D10 antibody, diluted 1/500 (cat #MA5-15511, Thermo Fisher Scientific). The WNT5A-L isoform was evaluated using a polyclonal rabbit antibody provided by Dr. Karl Willert, produced by immunizing a rabbit with a synthetic peptide of 18 amino acids corresponding to the difference on the amino-terminal end between the WNT5A-L and WNT5A-S isoforms (Bauer et al., 2013). In our lab, the rabbit serum was purified using the Melon™ Gel IgG Spin Purification kit (cat #45206, Thermo Scientific). The protein concentration was determined using the Pierce™ BCA Protein assay kit (cat #23225, Thermo Scientific). For IHC, we closely followed the protocol described in our previous publication (Saling et al., 2017). Briefly, 4-µm-thick sections from FFPE UC tissue samples were deparaffinized and antigen retrieval was performed using 10 mM citrate buffer, pH 6.0, for 30 minutes at 90°C. To block endogenous peroxidase, 3% H_2O_2 in phosphate-buffered saline (PBS) was applied to the sections for 15 minutes at room temperature. Primary antibodies for WNT5A, diluted in 1% bovine serum albumin (BSA) for the total/pan WNT5A antibody or to a concentration of 7.5 µg/mL in 1% normal goat serum in PBS for the WNT5A-L antibody, were applied to the samples for overnight incubation at 4°C. The isotype controls for each primary antibody, normal mouse IgG (ab18477, Abcam, Waltham, MA) and normal rabbit IgG (Invitrogen 10500C, Thermo Fisher Scientific), respectively, were applied under the same conditions on consecutive sections for each sample. The next day, after washing, a secondary goat anti-mouse (diluted 1/500, cat# sc-2031 Santa Cruz Biotechnology, Dallas, TX) or anti-rabbit (diluted 1/1,000, cat# ab97080 Abcam) antibody, each conjugated with horseradish peroxidase (HRP), was applied for 1 hour at room temperature. The substrate, diaminobenzidine (DAB) chromagen (Thermo Scientific), was applied and sections were then counterstained with hematoxylin, dehydrated, and a coverslip applied for immunostaining scoring. The degree or amount of staining was scored in a blinded

Table 1. Primer and Probe Details for dPCR and qPCR.

Oligo name	Oligo sequence (5'-3')	dPCR final conc (µM)	qPCR final conc (µM)
WNT5A-L fwd	TCGGGTGGCGACTTCCT	0.4	0.3
WNT5A-L probe	/5SUN/CGCCCCCTC/ZEN/CCCCTCGCCATGAAG/3IABkFQ/	0.05	
WNT5A-L rev*	CAACTCCTGGGCTTAATATTCCAAT	0.4	0.3
WNT5A-S fwd	CCTCTCGCCCATGGAATT	0.4	0.3
WNT5A-S probe	/56-FAM/CTGGCTCCA/ZEN/CTTGTTGCTCGGCC/3IABkFQ/	0.1	
WNT5A-S rev	GGGCTTAATATTCCAATGGACTTC		0.3

*Used in both L and S dPCR assays.

manner using a scale of 0 (no staining) to 3 (most intense staining).

Laser microdissection (LMD) / RT-qPCR

LMD and RNA extraction were performed on 10-µm-thick sections mounted onto Arcturus PEN membrane slides to collect tumor-rich regions for WNT5A mRNA expression quantification. Consecutive sections stained with HE served as a morphological reference for each sample. LMD membrane slides were stained using a special protocol where they were deparaffinized using xylene, rehydrated using decreasing ethanol concentrations, followed by distilled H_2O, hematoxylin, distilled H_2O, Scott's tap water, eosin, and then dehydrated with increasing ethanol concentrations and air dried. Sections of the biopsies that were primarily all tumor cells were selected and cut using the Leica DM 6000B microscope (Leica Biosystems, Deer Park, IL), pooling the dissected areas for a single patient sample into a tube for RNA isolation. The total area of the dissected tumor for each sample was recorded for

Table 2. Histopathological Features and Ratios of WNT5A-L and WNT5A-S RNA Expression in Human UC Samples.

	Histo-pathology		pathological staging				LMD/RT-PCR	ISH
Case	Grading	Histological pattern	Carcinoma *in situ* (Tis)	Non-invasive (pTa)	Lam propria invasion (pT1)	Muscle invasion (pT2)	WNT5A - L/S	WNT5A - L/S
1	Low	papillary	NR	+			29.4	22.4
2	Low	papillary	NR	+			1200.0	6.0
3	Low	papillary	NR	+			105.0	7.8
4	Low	papillary	NR		+		1400.0	3.1
5	Low	papillary/alveolar	NR	+			146.1	12.1
6	Low	papillary/inverted	Reported	+			14.4	53.3
7	High	papillary	NR		+		52/0	2.8
8	High	papillary	NR	+			421.4	9.1
9	High	papillary	NR	+			41/0	9.8
10	High	papillary	NR		+		2200.0	8.0
11	High	papillary	NR		+		25.9	2.2
12	High	papillary	NR	+			2.7	5.9
13	High	papillary	NR	+			6.3	7.6
14	High	solid	NR			+	2380.0	12.0
15	High	papillary/solid	NR		+		15.1	35.8
16	High	papillary/solid	NR		+		17.2	2.6
17	High	solid	NR			+	2/0	2.3

Tis, Carcinoma *in situ*; pTa, non-invasive carcinoma; pT1, tumor invades subepithelial connective tissue (lamina propria); T2, tumor invades muscularis propria. (NR) not reported; (+) present.

Table 3. LMD/RT-PCR and ISH Sample Summary.

		LMD / RT-PCR			ISH	
Case	Histological grade	Area	# of transcripts Long/unit area	# of transcripts Short/unit area	Average of transcripts Long/HPF	Average of transcripts Short/HPF
1	Low	1,911.698	206	7.01	124.00	5.55
2	Low	3,268.457	12	0.01	0.60	0.10
3	Low	3,665.294	19	0.18	17.70	2.50
4	Low	4,940.312	14	0.01	4.17	1.33
5	Low	3,508.096	57	0.39	15.70	1.30
6	Low	2,991.715	61	4.22	48.45	0.91
7	High	3,271.900	52	0	4.46	1.62
8	High	3,294.720	59	0.14	9.08	1.00
9	High	3,438.548	41	0	4.92	0.50
10	High	3,481.000	22	0.01	26.66	3.33
11	High	3,385.242	63	2.43	8.80	4.00
12	High	1,827.827	20	7.43	7.83	1.33
13	High	3,365.502	20	3.18	15.85	2.08
14	High	2,408.595	238	0.1	86.20	7.20
15	High	2,423.579	191	12.64	47.00	1.31
16	High	2,815.228	20	1.16	6.00	2.33
17	High	2,368.957	2	0	2.38	1.25

later normalization of the RNA expression as the number of RNA transcripts per unit area (Table 3). RNA was isolated from all 17 samples using a Qiagen FFPE miRNeasy kit (Germantown, MD), followed by cDNA synthesis using a High Capacity Reverse Transcription Kit plus RNase Inhibitor (Applied Biosystems, Foster City, CA). cDNA was amplified in triplicate using gene-specific primers (Table 1) and BioRad iTaq Universal SYBR Green Supermix (Hercules, CA) using a program of 95°C for 2 min and 50 cycles of 95°C for 10 sec and 60°C for 1 min followed by a melt curve analysis from 60°C to 95°C in a BioRad CFX384 Touch Real-Time PCR Detection System. The number of RNA transcripts for each isoform was determined using standard curves created from serial dilutions of quantified plasmids containing the targeted regions and then normalized against the total unit area of the dissected regions.

In situ hybridization (ISH)

Tissue sections (4 μm) from 17 FFPE blocks were used to examine the location and quantity of WNT5A-S and WNT5A-L isoform expression in UC human tissue samples. BaseScope Duplex Detection Reagent (Advanced Cell Diagnostics, Inc., Newark, CA) and custom probes designed to uniquely recognize the exon 1-exon 2 junction of each isoform RNA (#721261 BaseScope Probe BA-Hs-WNT5A-tv1-E1E2 targeting 639-674 of NM_003392.4 for WNT5A-Long and #721271-C2 BaseScope Probe BA-Hs-WNT5A-tv2-E1E2-C2 targeting 39-78 of NM_001256105.1 for WNT5A-Short) were used for ISH, essentially as described by the manufacturer. Probes targeting the bacterial gene for dihydrodipicolinate reductase (dapB) and labeled as both green and red were included as negative controls (#700141 Advanced Cell Diagnostics); probes targeting the genes for peptidyl-prolyl cis-trans isomerase B (PPIB), labeled as green, and for the largest subunit of RNA polymerase II (POLR2A), labeled as red, were included as positive controls for RNA integrity (#700101 Advanced Cell Diagnostics). In short, three consecutive slices of human UC tissue samples were placed on a Super-Frost Plus slide (Thermo-Fisher Scientific) and dried overnight. The following day, the samples were deparaffinized and a series of pretreatments with hydrogen peroxide, antigen retrieval solution, and protease IV were performed. The samples were then hybridized with the custom-designed WNT5A isoform BaseScope probes, as well as the positive and negative control probes provided by the manufacturer, with each red-green pair on a separate section on the same slide, put through a series of signal amplification and detection reactions, counterstained with hematoxylin, and mounted for viewing. Each single RNA transcript appeared as a distinct dot of chromogen precipitate visualized using a Nikon eclipse 80i bright field microscope (Nikon Instruments Inc., Melville, NY). The counting of green (WNT5A-L) and red dots (WNT5A-S isoform expression), was performed blindly by two independent observers only on those fields in which the two positive control genes were expressed. The results were expressed as the average number of dots per high power field (HPF) for each sample.

Statistical analysis

UC cell line results were presented as the mean expression of the five separate culture experiments relative to NUC expression ±SE. Symbols, as described in the figure legend, designated significant differences by two-way analysis of variance (ANOVA) (Graph Pad Prism, ver. 9) followed by *post hoc* analysis using Sidak's multiple comparison test ($P<0.05$). For WNT5A isoforms in tissue sections measured by LMD-RT-qPCR, the number of RNA transcripts for each isoform was determined using a standard curve and then normalized against the unit area of each LMD. For ISH, the number of transcripts was counted (red and green dots counted separately) and then normalized per HPF for each sample. The percentage of transcripts of each isoform was calculated based on the average number of transcripts (short + long isoforms) per HPF for each sample. One-way ANOVA was used for comparing expression in low-grade vs. high-grade tumors and pTa vs. pT1 stages. For all analyses, $P<0.05$ was considered to be statistically significant.

Results

WNT5A isoform expression in UC cell lines

The mRNA expression of each WNT5A isoform in three UC cell lines and one NUC line is shown in Figure 1. The WNT5A-L isoform is the predominantly expressed isoform in urothelial cells. The level of WNT5A-L mRNA was highest in J82 UC cells, moderate in RT4 and NUC cells, and lowest in T24 UC cells, however, only J82 was significantly different from all others (Fig. 1). Expression of WNT5A-S mRNA was also higher in J82 UC cells in comparison with the other three cell lines but differences were not significant between cell lines. Comparison of WNT5A-L *versus* WNT5A-S expression within each cell line was only significantly different in the J82 cell line, though the ratio of WNT5A-L/WNT5A-S was highly variable between UC cell lines: 61 for NUC, 40 for RT4, 75 for J82, 5 for T24 (Fig. 1).

Human FFPE-TUR tissue sample characterization

The 17 human tissue samples included in the study were collected during the TUR procedure for diagnostic purposes. Based on the pathology report, six were classified as low grade and eleven as high grade (Table 2). Invasion into the lamina propria was reported in eight of the 17 samples; only two samples showed histological evidence of detrusor muscle invasion, and both were high histological grade UC. The patterns described

varied from papillary to solid, and some of the samples showed evidence of squamous differentiation (Table 2).

WNT5A protein expression in human FFPE-TUR tissue samples

As an approach to investigate the expression of WNT5A protein levels in the 17 UC tissue samples, two different antibodies were used for IHC. The results reproduced the findings previously published by our lab (Malgor et al., 2013; Saling et al., 2017), with representative images shown in Figure 2. The specific protein expression of the WNT5A-L isoform was evaluated using a polyclonal antibody (Bauer et al., 2013). The results using the rabbit polyclonal antibody for WNT5A-L were inconclusive for our criteria because no difference was found between the commercial monoclonal antibody clone 3D10 (Fig. 2C,G) and the rabbit polyclonal antibody (Fig. 2D,H).

WNT5A isoform mRNA expression in human FFPE-TUR tissue samples

The areas dissected using LMD for RNA extraction included only areas of the tumor visualized in the tissue samples. Both RNA isoforms were detected by RT-qPCR in all 17 samples. The mean numbers of transcripts determined in the triplicate reactions for each isoform in each low-grade or high-grade sample are shown in Figure 3A and Table 3. In all cases, the WNT5A-L isoform was in greater abundance than the WNT5A-S isoform, independent of the grade or stage of the tumor.

WNT5A isoform mRNA localization in human FFPE - TUR tissue samples

To visualize the expression of each WNT5A isoform at the cellular level, *in situ* hybridization was performed on the 17 TUR FFPE tissue samples using isoform-specific probes. The quantification of red dots (WNT5A-S) and green dots (WNT5A-L) showed similar trends to the LMD RT-qPCR results (compare Fig. 3B to 3A). Both isoforms were expressed in all 17 samples (see ISH results in Table 3), however, the number of isoform transcripts was much lower than the positive controls included in the study (Fig. 4B vs. D and F vs. H). In all cases, the average number of WNT5A-L transcripts was higher than that of WNT5A-S (Fig. 3, Table 3). However, variation in the expression levels of both isoforms was found between different areas within a tumor tissue sample (Fig. 5A,B); consequently, the ratio of WNT5A-L/WNT5A-S transcripts varied area to area within each sample (Fig. 5C). This result shows the heterogeneity of the expression of WNT5A isoforms among tumor cells. The ratio of WNT5A-L/WNT5A-S transcripts per HPF for all samples analyzed varied from 2.2 to 53.3 (Table 2).

Interestingly, when we analyzed the percentage of

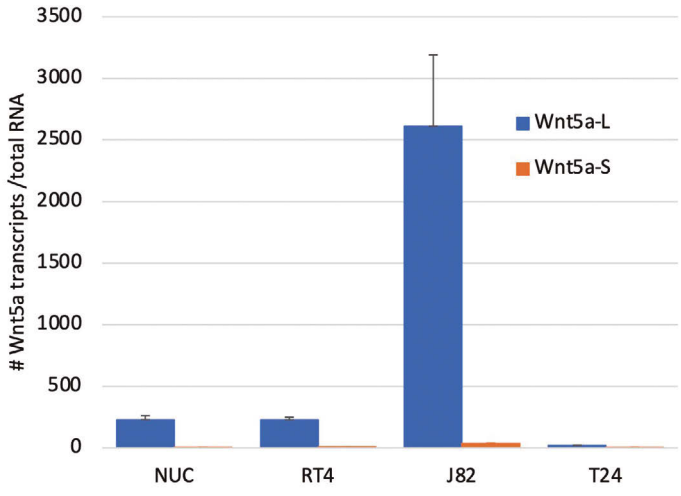

# Wnt5a-L	228.9	227.8	2612.1*	20.4
# Wnt5a-S	3.7	5.7	34.8	4.2
#L : #S	61	40	75^	5

* Significantly different from Wnt5a-L in other cell lines and from Wnt5a-S in same cell line (P<0.05)

^ Significantly different Wnt5a-L vs Wnt5a-S within J82 cell line (P<0.05)

Fig. 1. Wnt5a mRNA expression in four urothelial cell lines. The average number of transcripts of WNT5A-L and WNT5A-S isoforms per ng total RNA as determined by RT-dPCR as well as the ratio between Wnt5a-L and Wnt5a-S within each cell line is shown in the graph and/or the table below the graph. Two-way ANOVA (Graph Pad Prism, ver. 9) revealed the main effects of cell line and isoform and a significant interaction, but post hoc analysis using Sidak's multiple comparison test only revealed a significant difference (*) between WNT5A-L in J82 as compared with all other cell lines and (^) between Wnt5a-L vs. Wnt5a-S within the J82 cell line (N of five independent cultures per cell line; $P<0.05$).

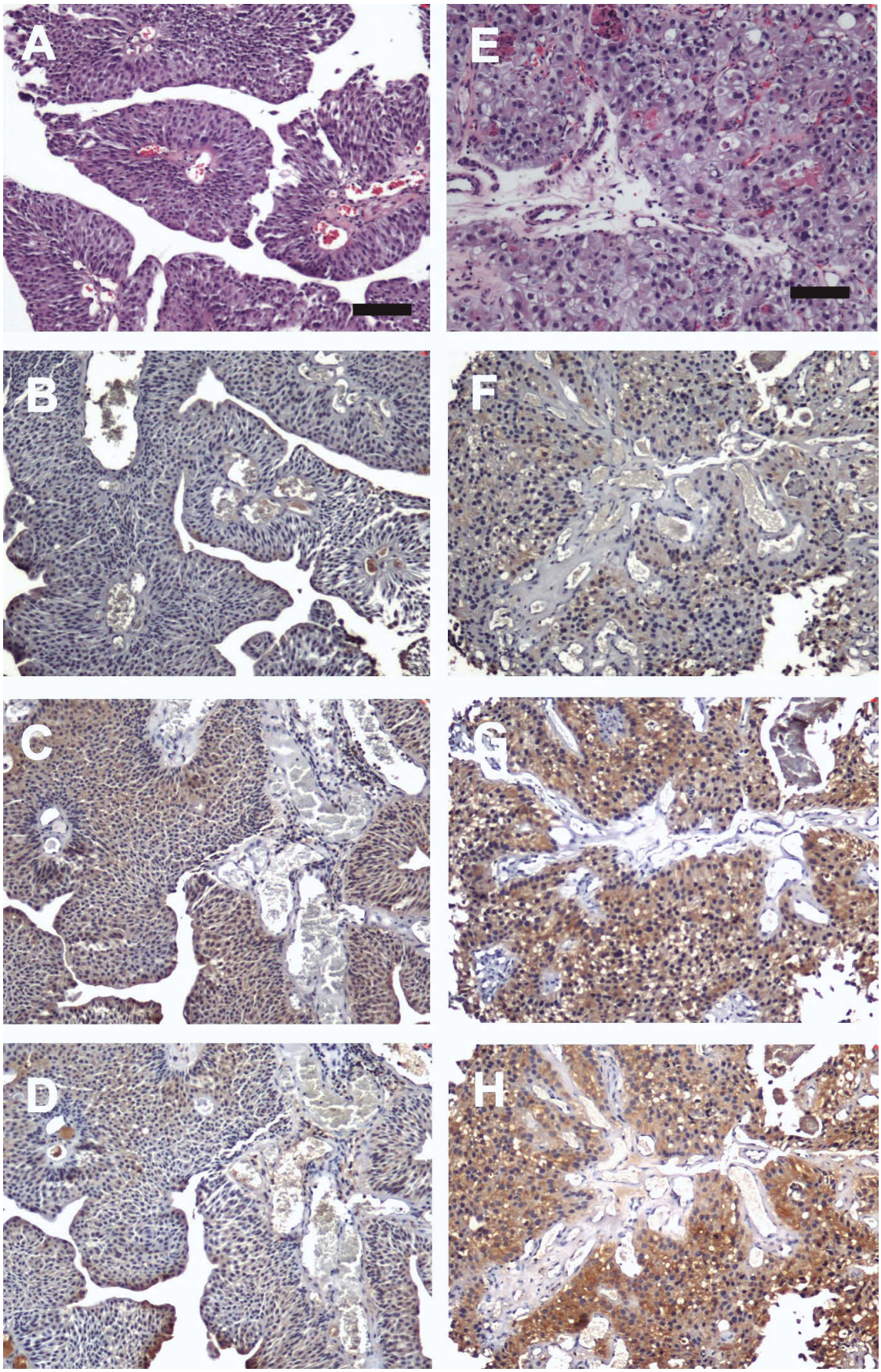

Fig. 2. Histological analysis of human low-grade **(A-D)** and High-Grade **(E-H)** UC Samples. **A, E.** Hematoxylin eosin staining. **B, F.** IHC isotype control. **C, G.** Expression of WNT5A using commercial monoclonal antibody clone 3D10. **D, H.** Expression of the WNT5A-L isoform using rabbit polyclonal antibody raised against a synthetic peptide of 18 amino acids from the amino-terminal end of the WNT5A-L isoform. All photos were taken using the 10X objective. Scale bars: 100 μm.

short isoform transcripts (red dots) per HPF with respect to the total number of transcripts (Long plus Short; green plus red) per HPF in each sample, there was a tendency for the percentage of WNT5A-S transcripts to be higher in high-grade *versus* low-grade tumors, with a median of 11.6% for high-grade tumors compared with 10.0% for low-grade tumors, although the difference was not statistically significant, P=0.25 (Fig. 6A). Surprisingly, when invasion into the lamina propria described in the pathology report was considered, the samples with lamina propria-invasion (pT1) showed a significantly higher percentage of WNT5A-S transcripts/HPF (Fig. 6B) and a lower percentage of WNT5A-L (Fig. 6C) than samples without invasion into the lamina propria (pTa).

Discussion

WNT5A signaling activation has been reported as an event involved in the pathogenesis of cancer, playing roles in cell proliferation, migration, invasion, and metastasis (Bo et al., 2013; Prasad et al., 2016; Bayerlova et al., 2017). Interestingly, opposite roles as tumor promoters or suppressors have also been reported for Wnt5a in different types of cancer (McDonald and Silver 2009; Chen et al., 2021). Expression of WNT5A has been reported in U but its mechanisms and functional roles are still unknown. Our group previously reported the expression of WNT5A protein and mRNA in UC cell lines and human UC tissue samples (Malgor et al., 2013; Saling et al., 2017). In the present work, we studied the expression of WNT5A-L and WNT5A-S isoforms in neoplastic urothelial cell lines and UC human tissue samples. The results revealed that both isoforms are expressed by a normal urothelial cell line, three neoplastic cell lines, and all 17 human UC tissue samples included in the study.

Our results revealed a predominance of WNT5A-L over WNT5A-S transcripts in the three neoplastic and one normal urothelial cell lines examined. As expected, due to its higher level of expression, WNT5A-L followed the same trend seen for total WNT5A previously reported for these cell lines by our lab (Saling et al., 2017). In addition, high variation in the expression of both isoforms was seen among the cell lines. This

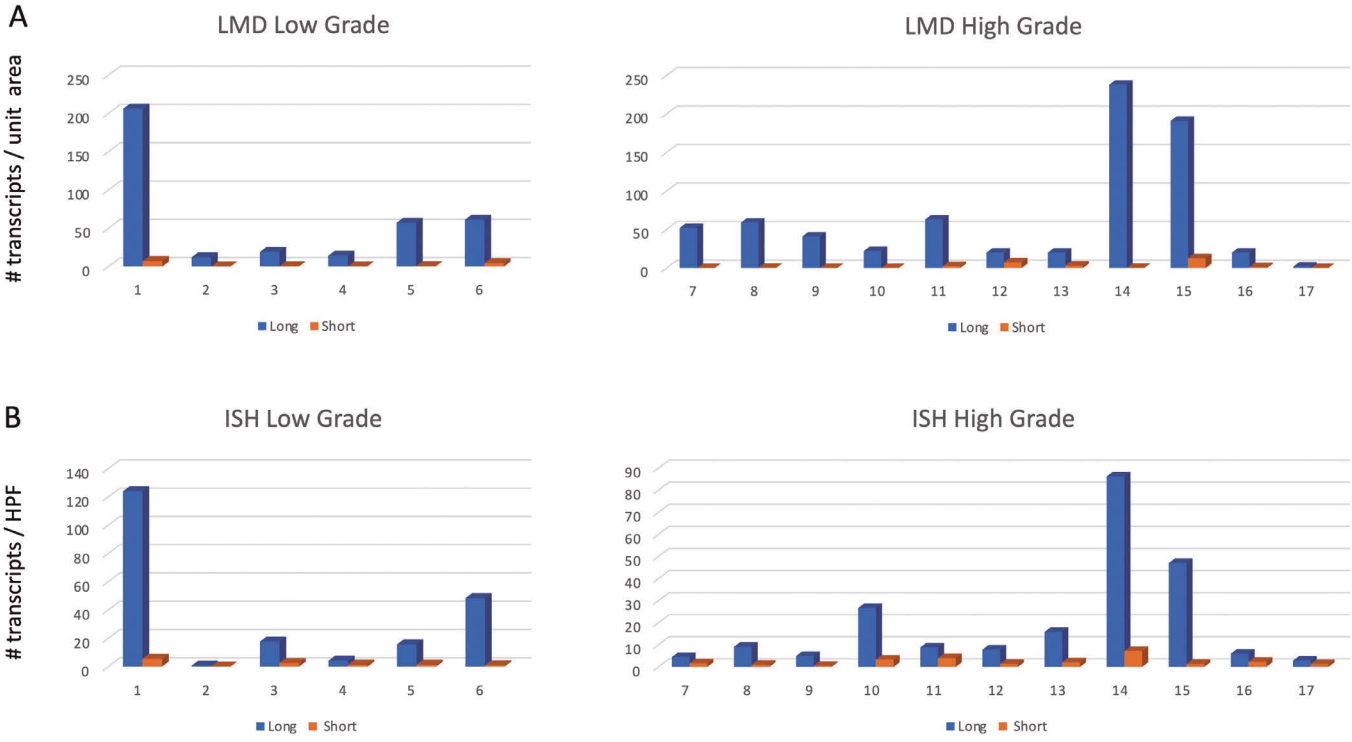

Fig. 3. Comparison of RT-qPCR Analysis and ISH Quantification of WNT5A Isoform Expression in Human UC Biopsy Samples. **A.** RT-qPCR quantification for each UC sample included in the study. Sequential biopsy sections were used for laser microdissection (LMD) to collect tumor-rich regions for RNA isolation and WNT5A quantification. RNA was isolated using the Qiagen miRNeasy FFPE kit (Germantown, MD), followed by cDNA synthesis. cDNA was amplified in triplicate using gene-specific primers. The number of RNA transcripts for each isoform was determined using a standard curve and then normalized against the unit area of each dissection. Graphs depict the mean number of transcripts determined in the triplicate reactions for each isoform in each low-grade (left, N of 6 samples) or high-grade (right, N of 11 samples) biopsy. **B.** ISH quantification for each UC sample included in the study. Graphs depict the mean number of transcripts determined per HPF for each isoform in each low-grade (left, N of 6 samples) or high-grade (right, N of 11 samples) biopsy.

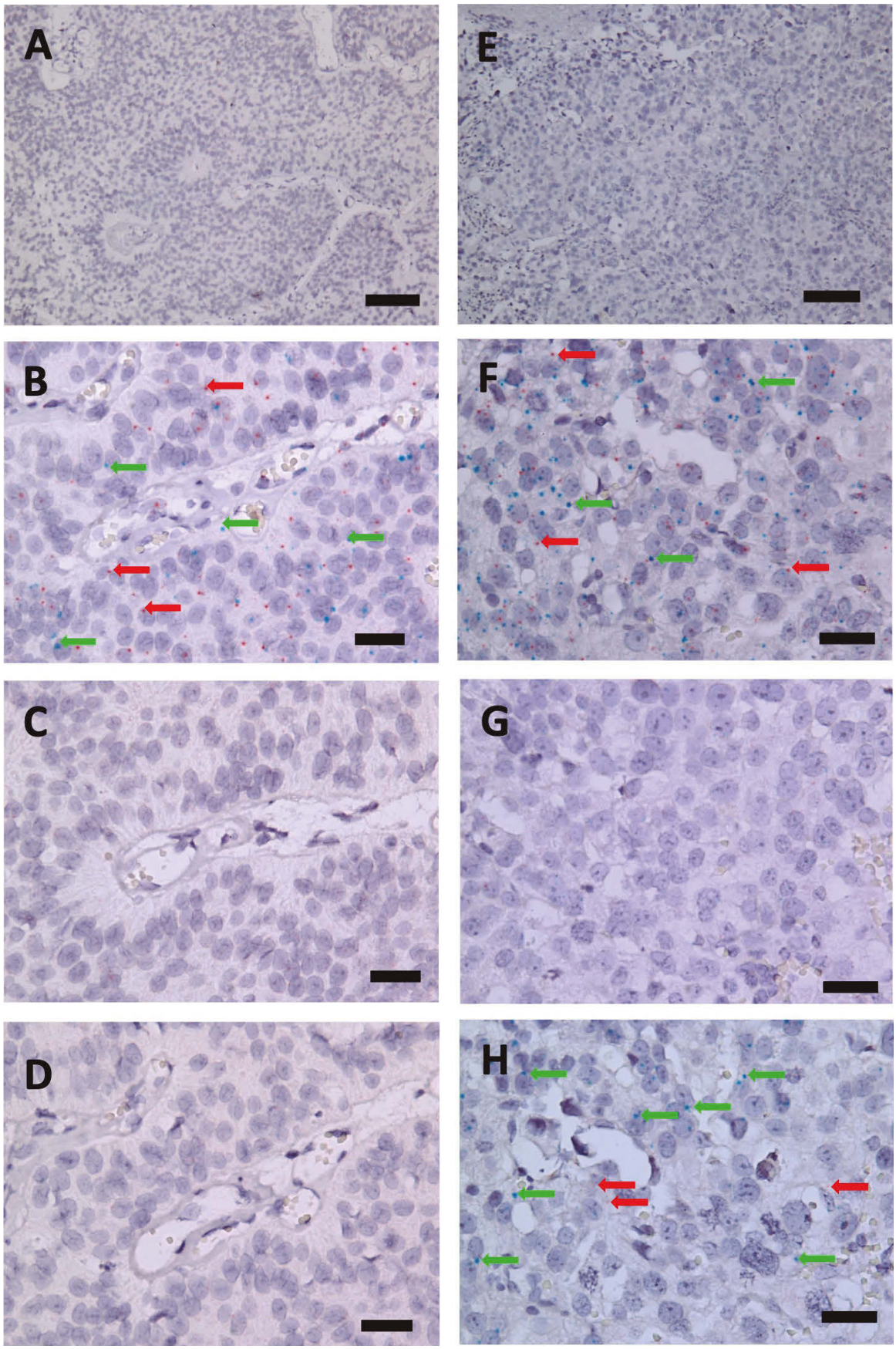

Fig. 4. *In situ* hybridization analysis of human low-grade **(A-D)** and high-grade **(E-H)** UC samples. **A, E.** Representative low-magnification (10 x) images of the samples. **B, F.** Positive control genes *PPIB* (green dots) and *POLR2A* (red dots) in the areas evaluated for the expression of WNT5A-S/WNT5A-L; **C, G.** Negative control dapB (green and red dots); **D, H.** Distribution of WNT5A-S (red dots) and WNT5A-L (green dots) at 40X magnification. Colored arrows indicate a few of the observed dots. Scale bars: A, E, 100 μm; B-D, F-H, 30 μm.

finding is in line with results reported by Bauer et al. that showed variable expression of both isoforms among several cancer cell lines (Bauer et al., 2013). Another study conducted by Huang et al. found relatively high mRNA expression of WNT5A-S in colorectal cancer cell lines, but they also found variable mRNA expression levels of WNT5A-S isoform among different cell lines (Huang et al., 2017). Finally, studies conducted by Katula et al. reported the expression of WNT5A-S and WNT5A-L isoforms in normal human osteoblast and two osteosarcoma cell lines (Vaidya et al., 2016; Bhandari et al., 2021). Interestingly, this study showed a decrease in transcripts from the promoter associated with the WNT5A-S isoform in the osteosarcoma cell lines compared with normal osteoblasts.

We also investigated the expression of both isoforms in human UC tissue samples, although the IHC results could not appreciably distinguish WNT5A-S from WNT5A-L protein expression. Since the only known difference between these two isoforms is an additional 18 amino acids at the N-terminus of WNT5A-L, the only isoform-specific antibody is one recognizing this unique N-terminus. The IHC, a semi-quantitative technique, using a WNT5A-L specific polyclonal antibody and a commercial monoclonal antibody recognizing an epitope within the common region of the WNT5A proteins, showed inconclusive results.

In contrast to the limitation of the IHC analysis, LMD/RT-qPCR and ISH analyses can exploit the unique differences in WNT5A RNA transcripts to specifically detect the unique first exon of each isoform (Bauer et al., 2013). Comparing our LMD/RT-qPCR and ISH results, we demonstrated relative agreement between the methods with regard to the expression of the specific WNT5A isoforms. Considering the entire tissue sample, isoform WNT5A-L was the predominant isoform in all 17 samples, independent of the histopathological features of the tumors; however, the ratio of WNT5A-L/WNT5A-S transcripts was highly variable among all UC tissue samples. Considering the results reported by Bauer et al., which showed only the expression of WNT5A-L isoform transcripts in normal bladder tissue, our results indicate that the transcription of the WNT5-S isoform may be associated with the presence of a pathological condition in the bladder (Bauer et al., 2013). Although we did not find a significant predominance of WNT5A-S mRNA expression over WNT5A-L mRNA in high-grade tumors as we initially expected, we did observe a trend of higher expression levels of WNT5A-S transcripts in high-grade tumors in comparison with low-grade tumors. Interestingly, the percentage of WNT5A-S transcripts was statistically higher in tumors with invasion into the lamina propria compared with those samples without invasion, as reported in the pathology report, while the percentage of WNT5A-L transcripts was statistically higher in tumors without invasion into the lamina propria. These findings suggest that WNT5A-S may be involved in an early step during the pathogenesis of UC by promoting the development of an invasive phenotype within the tumor, dividing tumors in pathological stage pTa from those in stage pT1. Further studies are needed to evaluate the possible application of WNT5A-S expression as a potential biomarker of early invasion and detection of

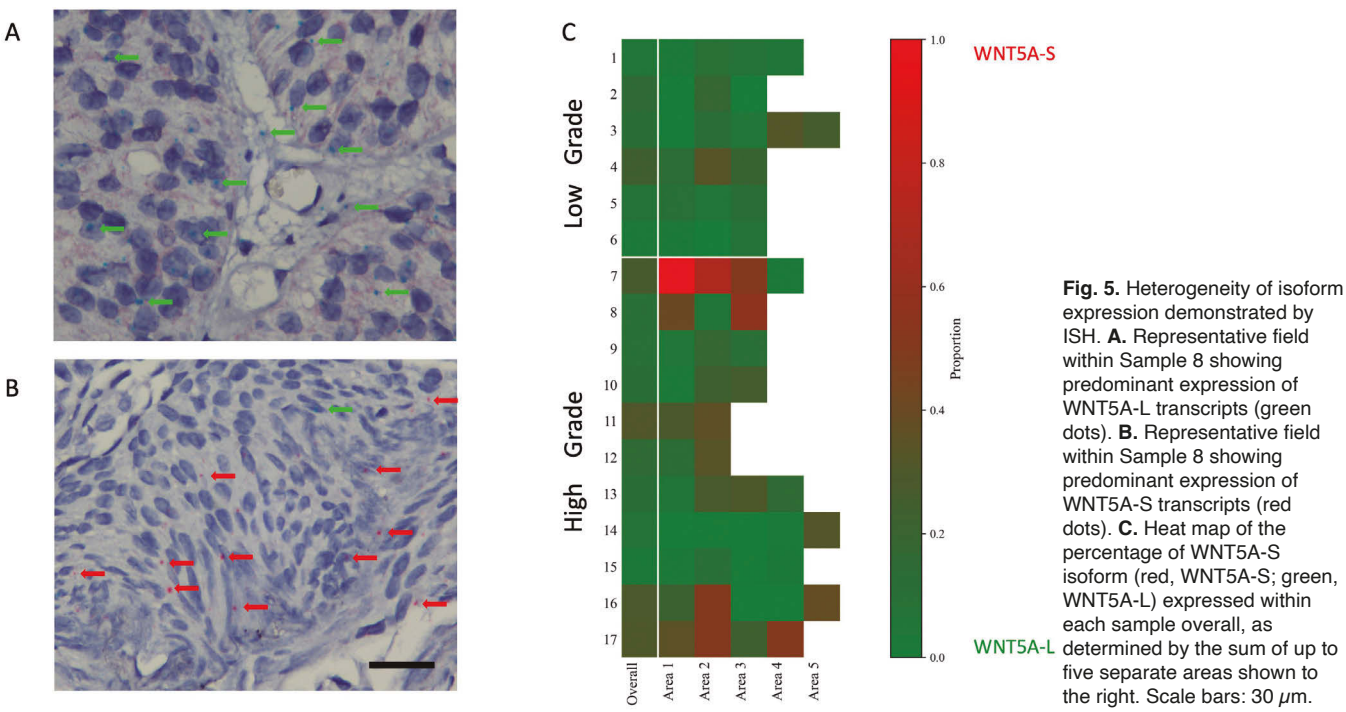

Fig. 5. Heterogeneity of isoform expression demonstrated by ISH. **A.** Representative field within Sample 8 showing predominant expression of WNT5A-L transcripts (green dots). **B.** Representative field within Sample 8 showing predominant expression of WNT5A-S transcripts (red dots). **C.** Heat map of the percentage of WNT5A-S isoform (red, WNT5A-S; green, WNT5A-L) expressed within each sample overall, as determined by the sum of up to five separate areas shown to the right. Scale bars: 30 μm.

early pT1-stage tumors. These findings are partly in agreement with results reported by Huang et al. who reported that a pattern of high WNT5A-S mRNA expression and low WNT5A-L mRNA expression correlated with the depth of colorectal cancer invasion (Huang et al., 2017). In this context, the invading role of WNT5A signaling in cancer has been previously reported for several types of cancers (Bachmann et al., 2005; Kurayoshi et al., 2006; Pukrop et al., 2006).

ISH results highlight some important findings with respect to the RNA expression of isoforms WNT5A-S and WNT5A-L: (a) Very low levels of RNA expression for both isoforms compared with the control genes *PPIB* and *POLR2A* were observed. This fact could be associated with differing transcriptional regulation or stability of transcripts as reported in different cancer types by other authors (Vaidya et al., 2016; Huang et al., 2017); (b) high variability in the expression of both isoforms within the tissue sample was observed. Although the total amount of transcripts in all tumor samples was predominantly WNT5A-L, different fields within a tumor showed differing expression levels of each isoform. This fact could be associated with tumor heterogeneity and, in this sense, further studies are needed; and (c) finally, it seems that the relative proportion of WNT5A-L and WNT5A-S transcripts may be important rather than the absolute number of transcripts expressed. This issue also needs further studies. A limitation of our study is that it is descriptive, and future functional studies about the effect of both WNT5A isoforms in UC are needed.

It is known that WNT5A in cancer participates in diverse biological processes, such as senescence of cancer stem cells, inflammation in the tumor microenvironment, cell migration, and tumor invasion (Kurayoshi et al., 2006; Pukrop et al., 2006; Bo et al., 2013; Asem et al., 2016; Prasad et al., 2016; Chen et al., 2021). The discovery of two isoforms for WNT5A brought forward the idea that isoforms could explain the contradictory roles that WNT5A plays in carcinogenesis (McDonald and Silver 2009; Azbazdar et al., 2021). In this context, Bauer et al. showed the opposite function for both isoforms, with WNT5A-S increasing cell proliferation and WNT5A-L decreasing it, and the authors speculated that the two isoforms may regulate distinct alternative signaling pathways associated with their functions as a tumor suppressor or tumor promoter. (Bauer et al., 2013). Another group explored the functionally distinct roles of both WNT5A isoforms in normal osteoblast differentiation, with the authors concluding that the isoforms have distinct and overlapping functions during the process (Bhandari et al., 2021).

On the other side, urothelial carcinomas comprise a heterogeneous group of malignancies in which different histopathological phenotypes and molecular subtypes have been recognized. Recently, a report described six molecular subtypes among UC, each with specific pathways involved in their pathogenesis, which highlights the diversity of the disease (Tan et al., 2019). A recent transcriptomic analysis conducted on 834 non-muscle-invasive bladder cancer patients identified four classes of tumors, reflecting the heterogeneity in tumor biology and clinical outcomes (Lindskrog et al., 2021).

In this context, it seems complicated and challenging to dissect the roles of WNT5A in UC because, in

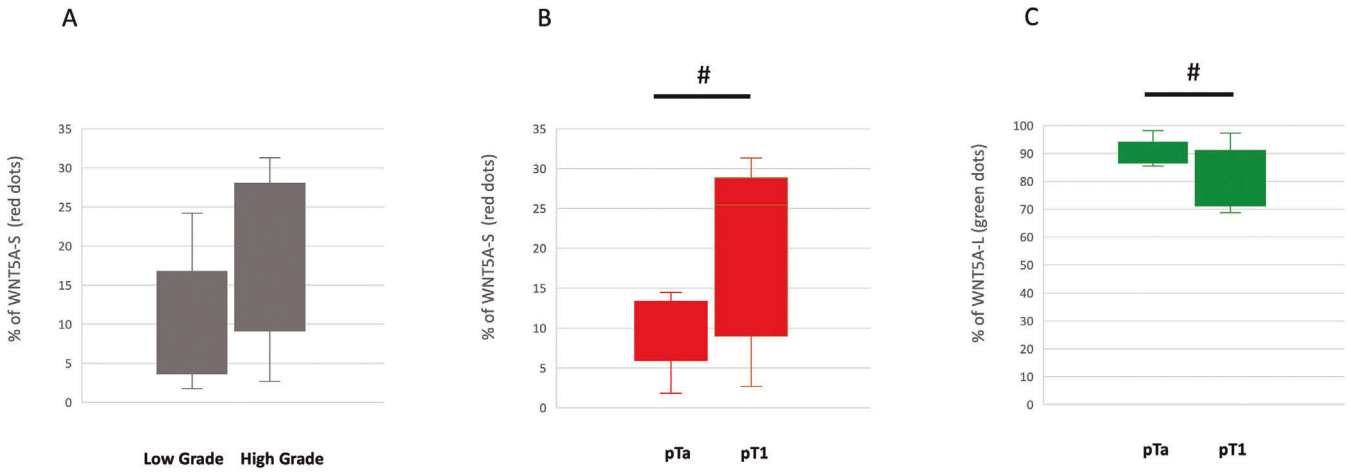

Fig. 6. Further Analysis of ISH on Human UC Samples. **A.** Distribution of the percentage of WNT5A-S transcripts in low and high histological grade UC tumors (low-grade, LG and high-grade, HG). The range of distribution is wide within each group and, although the median percentage of WNT5A-S transcripts is higher in the group of high-grade UC tumors (n= 11) than that of low-grade tumors (n=6), the difference is not significant. **B.** Distribution of percentage of WNT5A-S transcripts in UC samples with no lamina propria invasion (non-inv) vs. with lamina propria invasion (inv). The difference in the percentage of WNT5A-S (red dots) is statistically significant (*P*=0.01) between these two groups. **C.** Distribution of the percentage of WNT5A-L transcripts (green dots) in UC samples with no lamina propria invasion vs. with lamina propria invasion. The difference in the percentage of WNT5A-L (green dots) is statistically significant (#, *P*=0.01) between these two groups. Statistical analysis was performed by one-way ANOVA.

addition to the complexity of WNT5A signaling itself, several studies reported the cross-talk between WNT5A signaling and other pathways, such as transcription factor SOX4 (Moran et al., 2019) or exosomal BCYRN1 (Zheng et al., 2021), which have been reported to be regulators of WNT5A gene expression in UC. To overcome this issue, and determine the value of WNT5A isoforms as potential biomarkers to identify UC tumors in pTa *versus* pT1 or higher stages, future studies using a large number of samples including different histological subtypes and stages are needed.

In conclusion, our results show that both WNT5A-S and WNT5A-L isoforms are expressed in UC and suggest that a higher proportion of WNT5A-S transcripts compared with total WNT5A transcripts may be associated with lamina propria invasion. Also, the expression of both isoforms is not homogeneous within a tumor, indicating that future studies are needed to understand the transcription regulation of the WNT5A isoforms during UC oncogenesis in the context of tumor heterogeneity and tumor microenvironment.

Acknowledgements. The authors thank Dr Karl Willert for providing the rabbit polyclonal antibody.

We are grateful for the technical support provided by Ohio University's Histology Core Facility.

Conflict of interest. The authors have no conflict of interest.

Funding information. The study was funded in part by the Office of Research and Grants, Heritage College of Osteopathic Medicine, Ohio University.

Ethical statement. The study was conducted according to ethical principles approved by Ohio University IRB protocol #07E112. Informed Consent N/A, The Office of Research Compliance at Ohio University determined that this research meets the criteria for exempt category 4(ii) - secondary research for which consent is not required.

Registration of the study/trial, N/A. Animal studies, N/A

Author contributions. Conceptualization and design of experiments: K. Coschigano and R. Malgor. Experiments and data collection: A. Strope, C. Phillips, and S. Khadgi. Data analysis: A. Strope, S. Khadgi, K. Coschigano, and R. Malgor. Contribution of reagents and materials: A. Strope, C. Phillips, S. Jenkinson, K. Coschigano, and R. Malgor. Writing: K. Coschigano, and R. Malgor.

References

Ackers I., Szymanski C., Silver M.J. and Malgor R. (2020). Oxidized low-density lipoprotein induces WNT5A signaling activation in THP-1 derived macrophages and a human aortic vascular smooth muscle cell line. Front. Cardiovasc. Med. 7, 567837.

Asem M.S., Buechler S., Wates R.B., Miller D.L. and Stack M.S. (2016). Wnt5a signaling in cancer. Cancers (Basel) 8, 79.

Azbazdar Y., Karabicici M., Erdal E. and Ozhan G. (2021). Regulation of wnt signaling pathways at the plasma membrane and their misregulation in cancer. Front. Cell Dev. Biol. 9, 631623.

Bachmann I.M., Straume O., Puntervoll H.E., Kalvenes M.B. and Akslen L.A. (2005). Importance of P-cadherin, beta-catenin, and Wnt5a/frizzled for progression of melanocytic tumors and prognosis in cutaneous melanoma. Clin. Cancer Res. 11, 8606-8614.

Barker N. and Clevers H. (2006). Mining the Wnt pathway for cancer therapeutics. Nat. Rev. Drug Discov. 5, 997-1014.

Bauer M., Benard J., Gaasterland T., Willert K. and Cappellen D. (2013). WNT5A encodes two isoforms with distinct functions in cancers. PLoS One 8, e80526.

Bayerlova M., Menck K., Klemm F., Wolff A., Pukrop T., Binder C., Beissbarth T. and Bleckmann A. (2017). Ror2 signaling and its relevance in breast cancer progression. Front. Oncol. 7, 135.

Bhandari D., Elshaarrawi A. and Katula K.S. (2021). The human WNT5A isoforms display similar patterns of expression but distinct and overlapping activities in normal human osteoblasts. J. Cell. Biochem. 122, 1262-1276.

Bhatt P.M. and Malgor R. (2014). Wnt5a: A player in the pathogenesis of atherosclerosis and other inflammatory disorders. Atherosclerosis 237, 155-162.

Blumenthal A., Ehlers S., Lauber J., Buer J., Lange C., Goldmann T., Heine H., Brandt E. and Reiling N. (2006). The Wingless homolog WNT5A and its receptor Frizzled-5 regulate inflammatory responses of human mononuclear cells induced by microbial stimulation. Blood 108, 965-973.

Bo H., Zhang S., Gao L., Chen Y., Zhang J., Chang X. and Zhu M. (2013). Upregulation of Wnt5a promotes epithelial-to-mesenchymal transition and metastasis of pancreatic cancer cells. BMC Cancer 13, 496.

Cao J., Wang Q., Wu G., Li S. and Wang Q. (2018). miR-129-5p inhibits gemcitabine resistance and promotes cell apoptosis of bladder cancer cells by targeting Wnt5a. Int. Urol. Nephrol. 50, 1811-1819.

Chen Y., Chen Z., Tang Y. and Xiao Q. (2021). The involvement of noncanonical Wnt signaling in cancers. Biomed. Pharmacother. 133, 110946.

Costa V.L., Henrique R., Ribeiro F.R., Carvalho J.R., Oliveira J., Lobo F., Teixeira M.R. and Jeronimo C. (2010). Epigenetic regulation of Wnt signaling pathway in urological cancer. Epigenetics 5, 343-351.

Garg M. and Maurya N. (2019). WNT/β-catenin signaling in urothelial carcinoma of bladder. World J. Nephrol. 8, 83-94.

Geng M., Cao Y.C., Chen Y.J., Jiang H., Bi L.Q. and Liu X.H. (2012). Loss of Wnt5a and Ror2 protein in hepatocellular carcinoma associated with poor prognosis. World J. Gastroenterol. 18, 1328-1338.

Gordon M.D. and Nusse R. (2006). Wnt signaling: Multiple pathways, multiple receptors, and multiple transcription factors. J. Biol. Chem. 281, 22429-22433.

Hasan A., Mohammed Y., Basiony M., Hanbazazh M., Samman A., Abdelaleem M.F., Nasr M., Abozeid H., Mohamed H.I., Faisal M., Mohamed E., Ashmawy D., Tharwat M., Morsi D.F., Farag A.S., Ahmed E.M., Aly N.M., Abdel-Hamied H.E., Salama D.E.A. and Mandour E. (2023). Clinico-pathological features and immunohistochemical comparison of p16, p53, and ki-67 expression in muscle-invasive and non-muscle-invasive conventional urothelial bladder carcinoma. Clin. Pract. 13, 806-819.

Hausmann G., Banziger C. and Basler K. (2007). Helping Wingless take flight: How WNT proteins are secreted. Nat. Rev. Mol. Cell Biol. 8, 331-336.

Huang T.C., Lee P.T., Wu M.H., Huang C.C., Ko C.Y., Lee Y.C., Lin D.Y., Cheng Y.W. and Lee K.H. (2017). Distinct roles and differential expression levels of Wnt5a mRNA isoforms in colorectal cancer cells. PLoS One 12, e0181034.

Humphrey P.A., Moch H., Cubilla A.L., Ulbright T.M. and Reuter V.E. (2016). The 2016 WHO classification of tumours of the urinary

system and male genital organs-part b: Prostate and bladder tumours. Eur. Urol. 70, 106-119.

Katoh M. and Katoh M. (2009). Transcriptional mechanisms of WNT5A based on NF-kappaB, Hedgehog, TGFbeta, and Notch signaling cascades. Int. J. Mol. Med. 23, 763-769.

Katula K.S., Joyner-Powell N.B., Hsu C.-C.and Kuk A. (2012). Differential regulation of the mouse and human Wnt5a alternative promoters A and B. DNA Cell Biol. 31, 1585-1597.

Kumawat K. and Gosens R. (2016). WNT-5A: Signaling and functions in health and disease. Cell. Mol. Life Sci. 73, 567-587.

Kurayoshi M., Oue N., Yamamoto H., Kishida M., Inoue A., Asahara T., Yasui W. and Kikuchi A. (2006). Expression of Wnt-5a is correlated with aggressiveness of gastric cancer by stimulating cell migration and invasion. Cancer Res. 66, 10439-10448.

Le P.N., McDermott J.D. and Jimeno A. (2015). Targeting the Wnt pathway in human cancers: Therapeutic targeting with a focus on OMP-54F28. Pharmacol. Ther. 146, 1-11.

Lindskrog S.V., Prip F., Lamy P., Taber A., Groeneveld C.S., Birkenkamp-Demtröder K., Jensen J.B., Strandgaard T., Nordentoft I., Christensen E., Sokac M., Birkbak N.J., Maretty L., Hermann G.G., Petersen A.C., Weyerer V., Grimm M.O., Horstmann M., Sjödahl G., Höglund M., Steiniche T., Mogensen K., de Reyniès A., Nawroth R., Jordan B., Lin X., Dragicevic D., Ward D.G., Goel A., Hurst C.D., Raman J.D., Warrick J.I., Segersten U., Sikic D., van Kessel K.E.M., Maurer T., Meeks J.J., DeGraff D.J., Bryan R.T., Knowles M.A., Simic T., Hartmann A., Zwarthoff E.C., Malmstrom P.U., Malats N., Real F.X. and Dyrskjøt L. (2021). An integrated multi-omics analysis identifies prognostic molecular subtypes of non-muscle-invasive bladder cancer. Nat. Commun. 12, 2301.

Magers M.J., Lopez-Beltran A., Montironi R., Williamson S.R., Kaimakliotis H.Z. and Cheng L. (2019). Staging of bladder cancer. Histopathology 74, 112-134.

Malgor R., Crouser S., Greco D., Brockett C., Coschigano K., Nakazawa M. and Jenkinson S. (2013). Correlation of Wnt5a expression with histopathological grade/stage in urothelial carcinoma of the bladder. Diagn. Pathol. 8, 139.

McDonald S.L. and Silver A. (2009). The opposing roles of Wnt-5a in cancer. Br. J. Cancer 101, 209-214.

Mikels A.J. and Nusse R. (2006a). Wnts as ligands: Processing, secretion and reception. Oncogene 25, 7461-7468.

Mikels A.J. and Nusse R. (2006b). Purified Wnt5a protein activates or inhibits beta-catenin-TCF signaling depending on receptor context. PLoS Biol. 4, e115.

Miyazaki J. and Nishiyama H. (2017). Epidemiology of urothelial carcinoma. Int. J. Urol. 24, 730-734.

Moran J.D., Kim H.H., Li Z. and Moreno C.S. (2019). SOX4 regulates invasion of bladder cancer cells via repression of WNT5a. Int. J. Oncol. 55, 359-370.

Ng L.F., Kaur P., Bunnag N., Suresh J., Sung I.C.H., Tan Q.H., Gruber J. and Tolwinski N.S. (2019). WNT signaling in disease. Cells 8, 826.

Powles T., Bellmunt J., Comperat E., De Santis M., Huddart R., Loriot Y., Necchi A., Valderrama B.P., Ravaud A., Shariat S.F., Szabados B., van der Heijden M.S., Gillessen S. and ESMO Guidelines Committe (clinicalguidelines@esmo.org) (2022). Bladder cancer: ESMO clinical practice guideline for diagnosis, treatment and follow-up. Ann. Oncol. 33, 244-258.

Prasad C.P., Chaurasiya S.K., Guilmain W. and Andersson T. (2016). WNT5A signaling impairs breast cancer cell migration and invasion via mechanisms independent of the epithelial-mesenchymal transition. J. Exp. Clin. Cancer Res. 35, 144.

Pukrop T., Klemm F., Hagemann T., Gradl D., Schulz M., Siemes S., Trumper L. and Binder C. (2006). Wnt 5a signaling is critical for macrophage-induced invasion of breast cancer cell lines. Proc. Natl. Acad. Sci. USA 103, 5454-5459.

Saling M., Duckett J.K., Ackers I., Coschigano K., Jenkinson S. and Malgor R. (2017). Wnt5a/planar cell polarity signaling pathway in urothelial carcinoma, a potential prognostic biomarker. Oncotarget 8, 31655-31665.

Santini D., Banna G.L., Buti S., Isella L., Stellato M., Roberto M. and Iacovelli R. (2023). Navigating the rapidly evolving advanced urothelial carcinoma treatment landscape: Insights from italian experts. Curr. Oncol. Rep. 25, 1345-1362.

Siegel R.L., Miller K.D., Wagle N.S. and Jemal A. (2023). Cancer statistics, 2023. CA Cancer J. Clin. 73, 17-48.

Sung H., Ferlay J., Siegel R.L., Laversanne M., Soerjomataram I., Jemal A. and Bray F. (2021). Global cancer statistics 2020: GLOBOCAN estimates of incidence and mortality worldwide for 36 cancers in 185 countries. CA Cancer J. Clin. 71, 209-249.

Tan T.Z., Rouanne M., Tan K.T., Huang R.Y. and Thiery J.P. (2019). Molecular subtypes of urothelial bladder cancer: Results from a meta-cohort analysis of 2411 tumors. Eur. Urol. 75, 423-432.

Urakami S., Shiina H., Enokida H., Kawakami T., Tokizane T., Ogishima T., Tanaka Y., Li L.C., Ribeiro-Filho L.A., Terashima M., Kikuno N., Adachi H., Yoneda T., Kishi H., Shigeno K., Konety B.R., Igawa M. and Dahiya R. (2006). Epigenetic inactivation of Wnt inhibitory factor-1 plays an important role in bladder cancer through aberrant canonical Wnt/beta-catenin signaling pathway. Clin. Cancer Res. 12, 383-391.

Vaidya H., Rumph C. and Katula K.S. (2016). Inactivation of the WNT5A alternative promoter B is associated with DNA methylation and histone modification in osteosarcoma cell lines U2OS and SaOS-2. PLoS One 11, e0151392.

Zheng H., Chen C., Luo Y., Yu M., He W., An M., Gao B., Kong Y., Ya Y., Lin Y., Li Y., Xie K., Huang J. and Lin T. (2021). Tumor-derived exosomal BCYRN1 activates WNT5A/VEGF-C/VEGFR3 feedforward loop to drive lymphatic metastasis of bladder cancer. Clin. Transl. Med. 11, e497.

Accepted February 23, 2024